Journal of Inorganic Biochemistry 272 (2025) 113011

Contents lists available at ScienceDirect

Journal of Inorganic Biochemistry

journal homepage: www.elsevier.com/locate/jinorgbio

Cluster occupancy- and oxidation state-dependence of *Yersinia enterocolitica* IscR DNA binding☆

Elizabeth Gray, Miaomiao Gao, Justin M. Bradley, Jason C. Crack, Nick E. Le Brun *

Centre for Molecular and Structural Biochemistry, School of Chemistry, Pharmacy and Pharmacology, University of East Anglia, Norwich Research Park, Norwich NR4 7TJ, UK

ARTICLE INFO

Keywords:
Iron-sulfur cluster
Iron
Sulfide
Regulation
DNA binding
Mass spectrometry

ABSTRACT

Iron-sulfur (Fe–S) clusters are protein cofactors essential for life. Their assembly requires dedicated cellular machineries, such as the ISC system, found in *Escherichia coli* and many other bacteria. ISC is regulated by IscR, a member of the Rrf2 family of transcriptional regulators. *E. coli* IscR (*Ec*IscR) binds a [2Fe–2S] cluster and, in this form, functions as a repressor of the *isc* operon. Under aerobic conditions there is an increased cellular demand for Fe–S clusters, and apo IscR accumulates resulting in upregulation of ISC. Currently, the signal that *Ec*IscR directly responds to is not clear. Little is known about other IscR homologs and whether key functional features of the *E. coli* protein are broadly shared. Here, we report studies of the IscR homolog from the pathogen *Yersinia enterocolitica*. *Y. enterocolitica* IscR (*Ye*IscR) is ~80 % identical to *Ec*IscR and binds a [2Fe–2S] cluster most likely coordinated by three conserved Cys residues and one His. Isolated in the 1+ oxidation state, exposure to O_2 or other oxidants resulted in rapid oxidation of the cluster to the +2 state and slow cluster loss. The cluster was relatively insensitive to iron chelators, indicating that it is not labile. While the trigger for degradation of the *Ye*IscR cluster to generate the apo form is not clear, loss of the cluster resulted in a ~10-fold decrease in DNA affinity. The oxidation state of the cluster was found to be important for DNA binding, with a significant reduction in IscR-bound DNA observed upon oxidation, suggesting possible physiological importance.

1. Introduction

IscR regulates transcription of the iron-sulfur (Fe–S) cluster biogenesis (ISC) operon in many bacteria [1–6]. In *Escherichia coli*, IscR regulates both the ISC and SUF Fe–S cluster biogenesis machineries. A key feature is that, for a subset of IscR-regulated genes, DNA-binding activity is modulated through the occupancy of the Fe–S cluster site (referred to as type 1 sites). The *isc* operon is amongst this subset: when IscR is in its [2Fe–2S] cluster-bound form, binding to target DNA operator sequences is triggered, resulting in repression of transcription. When the cluster is absent, IscR affinity for the target sequence is decreased, causing de-repression of *isc* operon transcription [7]. Binding to type 2 site-regulated genes, which include the *suf* operon, is independent of the cluster.

In *E. coli*, it has been shown that several conditions, such as oxidative stress and low iron conditions, can cause a de-repression of the *isc* operon and therefore indicate loss of the [2Fe–2S] cluster from IscR [8–10]. The resulting apo form can bind DNA and activate *suf* expression, illustrating a complex, coordinated regulation of Fe–S cluster biogenesis in response to environmental conditions [11]. It is also becoming clear that IscR has a broader range of regulatory functions [7].

Yersinia are Gram-negative facultative anaerobes that are in some cases pathogenic in humans; in particular, *Y. pestis* is the causative agent of the plague, while *Y. enterocolitica* (principally) and *Y. pseudotuberculosis* are responsible for yersiniosis, an infectious disease of the gastrointestinal tract that mainly affects children [12]. It is also suggested that *Y. enterocolitica* may also play a role in Crohn's disease [13].

Abbreviations: CD, circular dichroism; EDTA, ethylenediaminetetraacetate; EMSA, electrophoretic mobility shift assay; ESI-MS, electrospray ionisation-mass spectrometry; Fe-S, iron-sulfur; HEPES, 4-(2-hydroxyethyl)piperazine-1-ethanesulfonic acid; ICP-MS, inductively coupled plasma-mass spectrometry; LC-MS, liquid chromatography-mass spectrometry; MWCO, molecular weight cut off; PMSF, phenylmethylsulfonyl fluoride; ROS, reactive oxygen species; SDS-PAGE, sodium dodecyl sulfate-polyacrylamide gel electrophoresis; SPR, surface plasmon resonance; Tris, tris(hydroxymethyl)aminoethane.

☆ This article is part of a Special issue entitled: 'Fe-S Proteins' published in Journal of Inorganic Biochemistry.

* Corresponding author.
E-mail address: n.le-brun@uea.ac.uk (N.E. Le Brun).

https://doi.org/10.1016/j.jinorgbio.2025.113011
Received 19 May 2025; Received in revised form 6 July 2025; Accepted 16 July 2025
Available online 22 July 2025

IscR in *Y. pseudotuberculosis* has been shown to be a regulator of the *isc* and *suf* operons, as observed in *E. coli*, as well as having broader roles. These include direct and indirect regulatory effects on the type III secretion system (T3SS) [14–16], utilised by *Yersinia* species to inject effector proteins, including virulence factors, into the host cell. IscR regulates the T3SS by controlling the regulator LcrF. Under aerobic or low-iron conditions, which the pathogen would be expected to experience once inside its host, IscR induces LcrF expression by binding to a type 2 site, and hence activates expression of the T3SS [15,16]. Deletion of the *iscR* gene in *Y. pseudotuberculosis* reduced virulence in mice, revealing an important role for IscR, and binding of apo IscR to the putative type 2 site in the *Y. pseudotuberculosis yscW-lcrF* promoter region was demonstrated [15]. Closely related IscR binding sites are found in other *Yersinia* species [14,16], and *Yersinia* IscR homologs are very highly conserved (Fig. S1), indicating a conserved regulatory role across the genus. Thus, it is important to understand how the DNA-binding activity of IscR is modulated in *Yersinia* species, *i.e.* the mechanism(s) that modulate [2Fe–2S] cluster stability and thus the balance between cluster-bound and apo forms of IscR.

So far, no *in vitro* studies of IscR proteins from *Yersinia* have been reported, providing motivation to determine similarities and differences to other characterised IscR proteins with respect to the nature of the Fe–S cluster and its stability in response to low iron or O_2/reactive oxygen species. Whilst understanding aspects of *Yersinia* IscR function is important, *Y. enterocolitica* IscR (*Ye*IscR) shares 80 % sequence identity with IscR from *E. coli*, suggesting that there must be shared functional features. Thus, studies of *Ye*IscR may also provide insight into the wider mechanism of cluster loss amongst IscR homologs. Here, we present *in vitro* studies of *Ye*IscR, demonstrating that it binds a [2Fe–2S] cluster that is relatively stable to O_2, and, in this form, binds IscR type 1 binding sites in a cluster occupancy- and oxidation state-dependent manner.

2. Materials and methods

2.1. Purification of Yersinia enterocolitica IscR and variants

Plasmids based on pGS-21a encoding C-terminal $(His)_6$-tagged IscR from *Yersinia enterocolitica*, and H107C and H107A variants of *Ye*IscR were purchased from Genscript. 8 × 2 L flasks containing 625 mL LB media with 100 mg/L ampicillin and 20 μM ferrous ammonium citrate were inoculated with *E. coli* strain BL21λDE3 harbouring the appropriate *Ye*IscR plasmid. Cultures were incubated at 37 °C and 200 rpm until OD_{600} = ~0.6, at which point protein expression was induced by the addition of 100 μM IPTG. To aid *in vivo* iron-sulfur cluster biogenesis, 200 μM ferrous ammonium citrate and 25 μM L-methionine were also added to the cultures. Cultures were then incubated at 37 °C and 105 rpm for 3.5 h before harvesting cells by centrifugation at 4500 rpm at 4 °C for 10 min. The cell pellets were washed with 50 mM Tris, 100 mM NaCl, 10 % (*v*/v) glycerol, pH 7.4 (buffer A), and then centrifuged at 8000 rpm at 4 °C for 10 min and pellets stored at −80 °C until purification.

All subsequent steps were performed in an anaerobic chamber unless otherwise stated (O_2 < 10 ppm). Pellets were resuspended in buffer A and 40 μg/mL lysozyme and 40 μg/mL phenylmethylsulfonyl fluoride (PMSF) added. The resuspended cells were removed from the anaerobic chamber, sonicated on ice, and returned to the anaerobic cabinet where the lysate was transferred to O-ring sealed centrifuge tubes, and centrifuged at 40,000 ×*g* for 45 min at 1 °C. The supernatant was then loaded onto 2 × 5 mL HisTrap™ FF (Cytiva) nickel affinity columns, previously equilibrated with buffer A, and the column washed with buffer A until the absorbance at 280 nm dropped to ~0.1. The bound protein was then eluted with an 80 mL buffer gradient, from 100 % buffer A to 20 % buffer A/80 % buffer B (buffer A containing 500 mM imidazole). The protein content was analysed by SDS-PAGE, and fractions containing *Ye*IscR were pooled and loaded onto a 5 mL HiTrap™ Heparin HP column (Cytiva), previously equilibrated with buffer A. The column was washed with buffer A until the absorbance at 280 nm dropped to ~0.1. The bound protein was manually eluted with 50 mM Tris, 1 M NaCl, 10 % (*v*/v) glycerol, pH 7.4, collected in 1.5 mL fractions and stored in an anaerobic fridge/freezer (at either 4 °C or − 35 °C, Belle or mBraun) until needed. Protein identity and purity was analysed by LC-MS and SDS-PAGE.

Concentrations of purified *Ye*IscR and variant proteins were determined using Rose Bengal dye [17] with absorbance of *Ye*IscR unknowns and standard BSA measured at 560 nm. Cluster concentrations were determined by ferene iron assay [18] or by using an iCAP-TQ inductively coupled plasma – mass spectrometer (ICP-MS, Thermofisher Scientific).

2.2. Spectroscopic experiments

UV–visible absorbance and circular dichroism (CD) spectra were recorded using a Jasco V550 spectrometer and a Jasco J810 spectropolarimeter, respectively. Samples were prepared and manipulated in an anaerobic glovebox (O_2 < 10 ppm) and measured between 260 and 900 nm (for absorbance) or 280–700 nm (for CD) in 1 cm pathlength anaerobic quartz cuvettes (Starna). For CD, two scans were recorded and averaged to improve the signal to noise ratio. Kinetic experiments for *Ye*IscR were performed by monitoring at 460 nm over 2000 s. Anaerobic experiments were performed in sealed cuvettes and prepared in the anaerobic glovebox. For O_2 experiments, protein samples were rapidly diluted with aerobic buffer A to give the desired O_2 concentration, and the cluster response immediately followed by spectroscopy.

2.3. Mass spectrometry measurements

For LC-MS, protein samples were prepared at a concentration of ~30 μM in 50 μL, and 450 μL LC-MS solvent (2 % (*v*/v) acetonitrile, 0.1 % (v/v) formic acid) was added to the sample. LC-MS was performed using an UltiMate 3000 HPLC system (Dionex) connected to the ESI source of a Bruker micrOTOF-QIII mass spectrometer (Bruker), calibrated with ESI-L Low Concentration Tuning Mix (Agilent Technologies). LC was operated through Chromeleon™ Chromatography Data System (CDS) Software (Thermo Scientific™). Briefly, a ProSwift™ RP-1S HPLC (Thermo Scientific™) column was washed with 15 % solvent A (0.1 % (*v*/v) formic acid in water), 85 % solvent B (0.1 % (v/v) formic acid in acetonitrile), then with 98 % solvent A and 2 % solvent B at a 0.2 mL/min flow rate. 20 μL of the sample was injected onto the column, and eluted using a 15-min linear solvent B gradient from 2 to 100 %, at a flow rate of 0.2 mL/min. A wash of 2 % (*v*/v) solvent B was run between each sample. Acquisition parameters for LC-MS were as follows: dry gas flow rate of 8.0 L/min, nebuliser pressure of 2.0 Bar, dry heater temperature 240 °C, capillary voltage 4500 V, end plate offset 500 V, collision cell RF 650 Vpp, between 50 and 3000 *m/z*.

The acquired mass spectrometry data was processed and analysed in Compass DataAnalysis version 4.1 (Bruker). Mass spectra were generated through using a maximum entropy deconvolution method over an appropriate mass range. Assignment of peaks was calculated from peaks corresponding to $[M + zH]/z$, where M is the molecular mass of the protein, H is the mass of the proton, and z is the charge of the ion ion [19]. Mass spectra are reported as relative intensity, where the maximum peak was arbitrarily set to 100 % and other peaks are reported as a percentage of this peak.

For native MS, *Ye*IscR samples were exchanged into 250 mM ammonium acetate pH 8.0 using a mini PD10 column (Cytiva). For simulation of low iron using an iron chelator, ethylenediaminetetraacetate (EDTA) was added to a final concentration of 0.5 mM to a solution of *Ye*IscR in 250 mM ammonium acetate pH 8.0. For investigation of *Ye*IscR binding to DNA, dsDNA oligonucleotides were prepared by mixing complementary forward and reverse strands (Table S1) to a final concentration of 50 μM. These were annealed for 10 min at 5 °C higher than the calculated melting point and allowed to cool. The annealed oligonucleotides were then exchanged into 100 mM ammonium acetate,

pH 8.0, using Zeba™ Spin Desalting Columns (ThermoFisher Scientific), with a 7 kDa molecular weight cut off (MWCO) and stored at −35 °C in an anaerobic chamber overnight. *Ye*IscR was exchanged into 1 M ammonium acetate to a final concentration of ~100 μM [2Fe–2S] *Ye*IscR using a mini PD10 column (Cytiva). *Ye*IscR was then diluted to a final concentration of 8 μM [2Fe–2S] in 100 mM ammonium acetate, pH 8.0, with the desired oligonucleotide added to the desired final concentration.

Samples were infused directly into the ESI source of a Bruker micrOTOF-QIII mass spectrometer (Bruker), operating in the positive ion mode and calibrated with ESI-L Low Concentration Tuning Mix (Agilent Technologies), at a flow rate of 0.3 mL/h. Mass spectra were typically acquired over 5–10 min, over a range of 1000–4000 *m/z*, using Bruker oTOF Control software (Bruker), with the following parameters: dry gas flow 4.0 L/min, nebuliser pressure 0.8 Bar, dry heater temperature 180 °C, capillary voltage 3500 V, end plate offset 500 V, ion energy 8.0 eV, collision cell RF 1500 Vpp, collision cell energy 10 eV.

The acquired mass spectrometry data was processed and analysed in Compass DataAnalysis version 4.1 (Bruker), or UniDec [20]. Mass spectra were generated through using a maximum entropy deconvolution method over an appropriate mass range, usually containing both the monomer and dimer masses within one deconvolution. Monomers and dimers can be distinguished within one deconvolution method by differences in their charge state profiles. For assignment of Fe–S cluster containing proteins, the mass of the Fe–S cluster peaks corresponds to to $[M + [FeS] + (z - x)H]/z$, where M is the molecular mass of the protein, $[Fe–S]^x$ is the mass of the Fe–S cluster with x charge, H is the mass of the proton, and z is the charge of the ion [19]. In this expression, the charge of the cluster, x, offsets the number of protons required to obtain an ion with z charge. The observed mass peak is usually offset from the predicted mass by the charge of the cluster, x, according to $[M + ([FeS] - x)]$ [19]. Mass spectra are reported as relative intensity, where the maximum peak was arbitrarily set to 100 % and other peaks are reported as a percentage of this peak.

2.4. Electrophoretic mobility shift assays (EMSAs)

An 80 bp DNA duplex of the *iscR* promoter region (p*iscR*) of *Y. enterocolitica*, containing two possible IscR binding sites (Table S2), with a 5′ 6-FAM label on the forward strand, was purchased from Eurofins Genomics. EMSA reactions were prepared on ice in 1× binding buffer (40 mM Tris, 30 mM KCl, pH 7.9), with 10 nM of the 80 bp p*iscR* fragment and varying concentrations of IscR. DNase-free water was added to a final volume of 20 μL. 2 μL of loading dye was added to the reactions (50 % (*v*/v) glycerol, 0.01 % (*w*/*v*) bromophenol blue) and reactions were incubated on ice for 2 min. 7.5 % (v/v) polyacrylamide gels were used for electrophoresis, as previously described [21]. The wells of the gel were flushed with 0.5× TBE buffer (45 mM Tris, 45 mM boric acid, 1 mM EDTA) and pre-run for 2 min at 30 mA. EMSA samples were run at 30 mA for 30 min and gels were visualised using an excitation wavelength of 473 nm on a GE Typhoon FLA 9000 Scanner (Cytiva). To generate apo *Ye*IscR, [2Fe–2S] *Ye*IscR was diluted to a final concentration of 30 μM with aerobic buffer A containing 5 mM EDTA and incubated for 90 min before exchanging into fresh, EDTA-free buffer.

2.5. Surface plasmon resonance (SPR)

ReDCaT SPR was used to study the interaction of YeIscR with DNA. Two 30-base oligonucleotides containing one of the IscR-binding sequences, termed site A and B, found in the *iscR* promoter region (p*iscR*) was purchased from Eurofins Genomics along with reverse complementary oligonucleotides that also contained a sequence complementary to the ReDCaT linker. Biotin ReDCaT linker oligonucleotides were also purchased (Table S3) [22]. The corresponding forward and reverse oligonucleotides (100 μM dsDNA) were annealed at 70 °C for 10 min and allowed to cool. Biotinylated dsDNA ReDCaT oligonucleotides were annealed to give 50 μM dsDNA and diluted to ~1 nM with SPR buffer (10 mM HEPES, 150 mM NaCl, 0.05 % polysorbate 20, pH 7.4) and captured on a strepavadin sensor chip (SAD200L, Xantec Bioanalytics GmbH) to a density of ~60 response units for all flow cells. Complementary ReDCaT oligonucleotides were then dissociated from working flow cells using regeneration buffer (50 mM NaOH, 1 M NaCl), and replaced with the dsDNA *iscR* promoter site A or site B sequence containing ReDCaT linker sequence on the complementary strand, as previously described [22,23].

SPR measurements were performed at 25 °C on a Biacore S200 system (Cytiva). To assess IscR interaction with the p*iscR* oligonucleotides, a multi cycle affinity methods protocol was run. *Ye*IscR was diluted under anaerobic conditions using SPR buffer to give 0–75 nM dimeric [2Fe–2S] IscR. Apo *Ye*IscR was prepared by mixing 5 mM EDTA with 30 μM *Ye*IscR under anaerobic conditions to prevent the formation of disulfide bridges between cysteine residues, and then diluted in SPR buffer to give 0–300 nM dimeric IscR. *Ye*IscR at variable concentration was injected on to the pre-prepared ReDCaT chip at 50 μL/min for 100 s to allow any protein to associate with the DNA. Buffer was then flowed over the flow cell for 100 s at 50 μL/min to allow any bound protein to dissociate. The chip was then regenerated between runs using 2 M NaCl in SPR buffer to disrupt protein-DNA interactions. Experiments were performed in triplicate for each protein concentration.

SPR sensorgrams were processed with Biacore evaluation software (Cytiva). At each concentration, the analyte response was normalised relative to the maximum observed response and then averaged, as previously described [23]. Relative response was plotted against the dimeric [2Fe–2S] concentration for holo proteins, or against the dimeric protein concentration for apo proteins, and fitted using a Hill equation:

$$Relative\ Response = R_{max}\left(x^n / K_d^n + x^n\right) \quad (1)$$

where R_{max} is the maximum relative response, x is the dimeric protein concentration, K_d is the dissociation constant, and n is the Hill coefficient. Fitting was performed in OriginPro, Version 2021b (OriginLab Corporation).

3. Results

3.1. As-isolated YeIscR binds a [2Fe–2S] cluster

C-terminally His-tagged *Yersinia enterocolitica* IscR (*Ye*IscR) was anaerobically purified following over expression in *E. coli*, resulting in a dark red solution. LC-MS revealed a major peak at 19,286 Da (Fig. S2A), which compares well with the predicted mass of *Ye*IscR at 19,285 Da. The spectrum contained a minor peak at +32 Da, indicative of a sulfur adduct, but no other species, consistent with SDS-PAGE (Fig. S2B). The UV–visible absorption spectrum contained maxima at 420 nm and 560 nm (Fig. 1A), typical of a [2Fe–2S] cluster-binding protein [24], and in agreement with previous work on IscR from *E. coli* [1,25]. Colorimetric iron assays and ICP-MS measurements indicated that incorporation of the [2Fe–2S] cluster into *Ye*IscR varied between 50 and 95 %, depending on the purification. Visible CD spectroscopy, which is particularly sensitive to the cluster environment, gave a spectrum (Fig. 1B) with a double negative peak at 360 nm and 380 nm, and an intense positive peak at around 470 nm.

Addition of an excess of sodium dithionite resulted in UV–visible absorbance and CD spectra similar to those of the as-isolated protein. Exposure of the sample to air for 30 min resulted in spectral changes, Fig. 1A and B, with a peak maximum in the absorption spectrum at 460 nm and loss of a distinct peak at 560 nm. In the CD spectrum, collapse of the double peak at 360/380 nm to a single, lower intensity peak at 370 nm was observed, along with almost complete loss of intensity at 470 nm and appearance of weak bands at 460 nm and 500 nm. Thus, both UV–visible absorption and CD spectra indicate that, as isolated, the

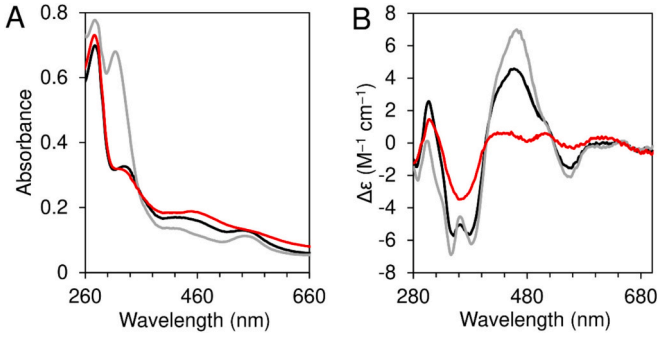

Fig. 1. Redox cycling of *Ye*IscR. Spectroscopic characterisation of *Ye*IscR by (A) UV–visible absorbance and (B) Circular dichroism spectroscopies, showing as-isolated *Ye*IscR (black), in the presence of 100 μM dithionite (grey) and after 30 min air oxidation (red). 30 μM *Ye*IscR in 50 mM Tris, 800 mM NaCl, 5 % (*v*/v) glycerol, pH 8.0. Spectroscopic measurements were performed in sealed 1 cm cuvettes. (For interpretation of the references to colour in this figure legend, the reader is referred to the web version of this article.)

*Ye*IscR [2Fe–2S] cluster was predominately in its reduced, $[2Fe–2S]^{1+}$, form after anaerobic purification from *E. coli*. Exposure to O_2 resulted in oxidation of the cluster to the $[2Fe–2S]^{2+}$ state. These observations are in agreement with those made previously for *E. coli* IscR [1,25].

The Fe–S cluster bound by *Ye*IscR was confirmed by electrospray ionisation mass spectrometry (ESI-MS) performed under native (non-denaturing) conditions. The *m/z* (Fig. S3) and deconvoluted spectra contained two major species, one at 19,459 Da, corresponding to monomeric [2Fe–2S] cluster-bound *Ye*IscR, and the other, at 38,919 Da, corresponding to the dimeric form of *Ye*IscR with two [2Fe–2S] clusters bound (Fig. 2). Observation of dimeric *Ye*IscR is consistent with reports on IscR proteins from *E. coli* and *T. potens* [26,27], as well as for other proteins from the Rrf2 family [28–31]. The presence of monomeric *Ye*IscR is likely due to the monomerisation of the protein during the ionisation process, as has been observed by native ESI-MS for other Rrf2 family regulators [28,32,33]. As in other cases, this was helpful in confirming the presence of a [2Fe–2S] cluster in each subunit. Predicted and observed masses are shown in Table 1.

3.2. His107 of YeIscR is likely a ligand of the [2Fe–2S] cluster

Previous work has suggested that the [2Fe–2S] cluster of *E. coli* IscR is coordinated by three cysteine residues and a histidine residue located close to the cysteines [25]. This is consistent with other studies of Fe–S cluster Rrf2 family regulators demonstrating non-cysteine cluster coordination [30,31]. The four proposed cluster ligands of *E. coli* IscR are conserved in *Y. enterocolitica* IscR (Fig. S4). To determine whether the histidine residue at position 107 of *Ye*IscR is involved in the ligation of the [2Fe–2S] cluster, H107C and H107A variants were generated and purified. LC-MS confirmed that observed masses match those predicted (H107C predicted mass 19,249 Da, observed 19,251 Da; H107A predicted mass 19,220 Da, observed 19,219 Da). As-isolated proteins contained very little or no cluster, as indicated by UV–visible absorption and CD spectroscopies (Fig. 3)), where all characteristic peaks between 400 and 600 nm observed for the wild-type protein were absent or greatly

Table 1
Predicted and observed masses for apo- and holo-forms of *Ye*IscR.

IscR species	Predicted mass (Da)	Observed mass (Da)	Mass difference (Da)
Monomeric			
Apo	19,285	19,284	−1
[2Fe–2S]	19,459	19,459	0
Zn	19,348	19,348	0
Dimeric			
Apo	38,570	–	–
[2Fe–2S]/[2Fe–2S]	38,918	38,919	1
[2Fe–2S]/Zn[a]	38,807	38,806	−1
[2Fe–2S]/2Zn[a]	38,870	38,871	+1

[a] ICP-MS analysis revealed the presence of Zn^{2+} in IscR preparations. Distinguishing between Zn^{2+} and sulfur (2 x S) adducts is problematic. The detection of peaks separated by 32 Da on the higher mass side of the doubly cluster-bound IscR dimer suggests that sulfur adducts may also contribute to these peaks assigned as cluster and Zn adducts.

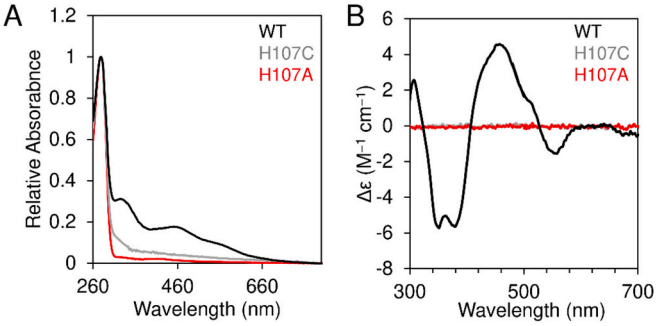

Fig. 3. Biophysical characterisation of *Ye*IscR cluster variants. (A) UV–visible absorbance and (B) CD spectroscopies of wild type (WT) *Ye*IscR (black), H107C (grey) and H107A (red). IscR proteins (30 μM) were in 50 mM Tris, 100 mM NaCl, 5 % (*v*/v) glycerol, pH 8.0, Measurements were performed in sealed 1 cm pathlength cuvettes. (For interpretation of the references to colour in this figure legend, the reader is referred to the web version of this article.)

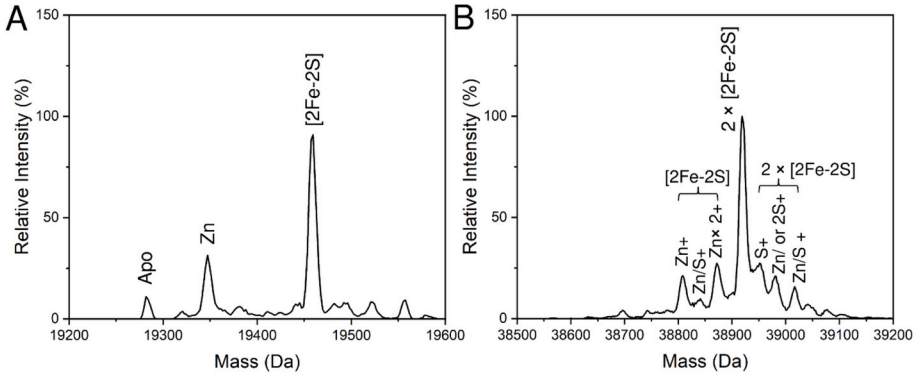

Fig. 2. Native ESI mass spectrometry of *Ye*IscR. Deconvoluted spectra of the monomeric region (A) and dimer region (B) of *Ye*IscR (30 μM) in anaerobic 250 mM ammonium acetate pH 8.0. In addition to cluster-bound forms, apo monomeric *Ye*IscR was also detected, along with sulfur adducts of *Ye*IscR (in both monomeric and dimeric regions).

reduced in intensity. This is consistent with an important role for His107 in cluster coordination in *Ye*IscR, and the previous conclusion from studies of the *E. coli* protein that His107 is the fourth cluster ligand [25].

3.3. The YeIscR [2Fe–2S] cluster degrades slowly under aerobic conditions

Fe–S cluster-binding proteins are commonly sensitive to O_2 and oxidative stress [34,35]. Indeed, the repression of IscR-regulated genes is alleviated under aerobiosis/oxidative stress [2,8,10,36], consistent with the idea that such conditions lead to the loss of the [2Fe–2S] cluster from the protein, and hence de-repression. However, it is currently unclear whether the IscR [2Fe–2S] cluster responds directly or indirectly to these signals. An indirect response could result, for example, from the general loss of cytoplasmic solvent-exposed Fe–S clusters under oxidative stress [37] and consequent prioritisation of cluster supply to such proteins over IscR, leading to accumulation of apo IscR. Therefore, the sensitivity of the [2Fe–2S] cluster of *Ye*IscR to O_2 and various reactive oxygen species (ROS) was investigated.

*Ye*IscR was diluted with aerobic buffer to give final concentrations of [2Fe–2S] cluster and O_2 of 30 and 210 μM, respectively, and UV–visible absorbance and CD spectra measured (Fig. 4). From both spectra, it was apparent that the [2Fe–2S] cluster was rapidly oxidised in the presence of O_2, within the timescale of the spectral measurement. This was characterised by a peak at 460 nm in the UV–visible absorbance spectrum and the loss of the double peak at 360/380 nm, and of intensity above 450 nm in the CD spectrum immediately after exposure to oxygenated buffer, referred to as time = 0 min. UV–visible absorbance and CD spectra were then recorded over time to monitor any further changes to, or degradation of, the [2Fe–2S] cluster. A gradual loss of UV–visible absorbance intensity at 460 nm was observed over a period of 8 h (Fig. 4A), indicative of a slow degradation of the [2Fe–2S] cluster, and similar loss of intensity was also observed by CD (Fig. 4B). Such a slow decay suggests that IscR may not be a direct sensor of O_2, or at least that O_2 alone is not sufficient to initiate the decay of the IscR cluster.

3.4. The YeIscR [2Fe–2S] cluster is resistant to hydrogen peroxide but sensitive to superoxide

Other reactive oxygen species (ROS) known to damage Fe–S cluster cofactors include hydrogen peroxide [38] and superoxide [37,39]. In *E. coli*, induction of the *isc* and *suf* operons in response to peroxide has been shown to be dependent on IscR [8,9], implying that peroxide can stimulate the conversion of [2Fe–2S] IscR to apo IscR. Additionally, some evidence suggests that the [2Fe–2S] cluster of *Pseudomonas aeruginosa* IscR may be sensitive to peroxide [40]. Therefore, the sensitivity of the *Ye*IscR [2Fe–2S] to peroxide and superoxide was tested.

The intracellular concentration of peroxide is predicted to be 20–50 nM under normal conditions, with 200 nM hydrogen peroxide being sufficient to induce the OxyR regulator in response to oxidative stress [39]. Hydrogen peroxide was added to *Ye*IscR under anaerobic conditions at a concentration equimolar to the [2Fe–2S] cluster (30 μM), a concentration more than sufficient to reflect any effect that may occur *in vivo*. Superoxide was generated *in situ* using 22 mU/mL xanthine oxidase with the addition of 1 mM hypoxanthine, as previously described [37]. The concentration of superoxide generated was determined to be 35 μM using a cytochrome *c* reduction assay, Fig. S5. The response of [2Fe–2S] IscR to peroxide and superoxide was monitored by UV–visible absorbance and/or CD spectroscopies, see Fig. S6 and Fig. 5, respectively.

In the case of peroxide, absorbance and CD changes occurred within the timeframe of the first measurement that were indicative of oxidation of the [2Fe–2S] cluster. Following this, degradation of the cluster was very slow, with very little change in absorbance at 460 nm observed over 180 min (Fig. S6)). In the case of superoxide, $A_{460\ nm}$ decreased slowly over a period of 420 min (Fig. 5). This experiment was performed aerobically, due to the requirement for O_2 by xanthine oxidase for superoxide production. There are differences observed in the decay of the [2Fe–2S] cluster in the presence of superoxide compared to O_2 alone (compare Figs. 4C and 5B), suggesting that superoxide does have an effect on the [2Fe–2S] cluster. However, these occur over a relatively long period of time, indicating that superoxide-mediated cluster degradation does not occur over a physiologically relevant time frame.

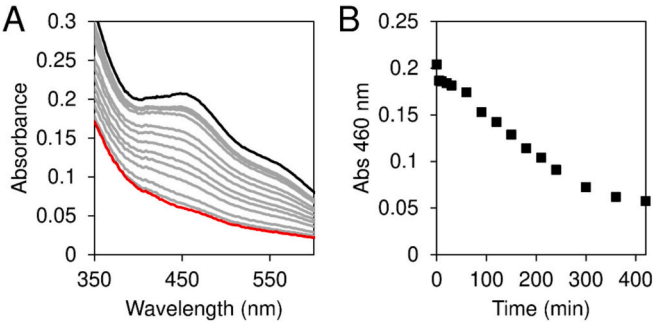

Fig. 5. *Ye*IscR [2Fe–2S] cluster sensitivity to superoxide. (A) UV–visible absorbance spectra of *Ye*IscR in response to superoxide between 0 min (black) and 420 min (red), intervening time points are shown in grey. (B) Absorbance at 460 nm over 420 min. 35 μM superoxide was generated under aerobic conditions using 22 mU/mL xanthine oxidase and 1 mM hypoxanthine. *Ye*IscR was diluted to final [2Fe–2S] concentration of 30 μM in 50 mM Tris, 1 M NaCl, 10 % (*v*/v) glycerol, pH 7.4. Spectroscopy performed in 1 cm pathlength cuvette. (For interpretation of the references to colour in this figure legend, the reader is referred to the web version of this article.)

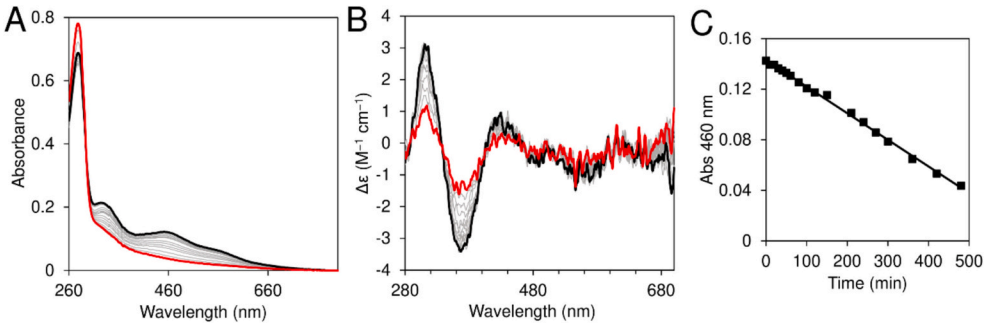

Fig. 4. Degradation of *Ye*IscR [2Fe–2S] cluster in the presence O_2. (A) UV–visible absorption and (B) CD spectra of [2Fe–2S] *Ye*IscR measured over time in response to O_2, between 0 min (black) and 470 min (red). Intervening time points are shown in grey. (C) Change in UV–visible absorbance at 460 nm over 470 min. *Ye*IscR was diluted to 30 μM in oxygenated buffer (50 mM Tris, 800 mM NaCl, 5 % (*v*/v) glycerol, pH 8.0). Spectroscopic measurements were recorded in 1 cm pathlength cuvettes. A linear fit of the 460 nm absorbance decay in (C) gave a decay rate of the [2Fe–2S] cluster of 0.00021 ΔA min^{-1}. (For interpretation of the references to colour in this figure legend, the reader is referred to the web version of this article.)

3.5. Response of YeIscR [2Fe–2S] to low iron conditions

Previous work has demonstrated that there is an increase in expression of IscR-regulated genes in *E. coli* under low iron conditions [8], implying that, *in vivo*, the [2Fe–2S] cluster of IscR is degraded. Therefore, the effect of low iron on the stability of the [2Fe–2S] cluster of *Ye*IscR was investigated. Ethylenediaminetetraacetate (EDTA) is a chelator with a high affinity for iron, with log *K* values of 14.3 and 25.1 for Fe^{2+} and Fe^{3+} respectively [41]. EDTA has previously been utilised to simulate low-iron conditions for *in vitro* stability experiments with another Fe–S cluster Rrf2 family member, RirA, which functions as an iron sensor [42]. To investigate whether the [2Fe–2S] cluster of *Ye*IscR senses iron through a related mechanism, EDTA was added to *Ye*IscR under anaerobic and aerobic conditions, and the response of the [2Fe–2S] cluster was monitored over time by UV–visible absorbance, Fig. S7A. Under anaerobic conditions, in response to EDTA, the cluster degraded relatively slowly over 240 min. Under aerobic conditions, degradation of the cluster was more rapid, with complete cluster loss observed within ~70 min. This is significantly more rapid than observed for O_2 alone (Fig. 4).

To gain further insight into the cluster degradation process under aerobic conditions, native ESI mass spectrometry was utilised to monitor the breakdown of the [2Fe–2S] cluster of *Ye*IscR in response to EDTA. Time-dependent measurements revealed the accumulation of the apo form, along with degradation products of the [2Fe–2S] cluster, such as [Fe–S] and [2Fe–S], as well as sulfur adducts of *Ye*IscR (Fig. S7B). However, masses that correspond to the Fe–S cluster breakdown products were only detected as EDTA-bound forms, which implies that a direct interaction is needed between EDTA and the [2Fe–2S] cluster for degradation to occur. Alternatively, it may be that EDTA-Fe complexes were non-specifically bound to apo *Ye*IscR. The observed Fe–S cluster breakdown products did not form and decay in an ordered way, such as was observed for the EDTA-mediated degradation of the [4Fe–4S] cluster of RirA [42], suggesting that once the cluster breakdown is initiated, the cluster does not degrade *via* one specific breakdown pathway, or that Fe–S species can re-associate with the protein, making elucidation of a distinct pathway difficult.

To determine whether the observed species in the mass spectra are due to a direct interaction between the [2Fe–2S] cluster of *Ye*IscR and EDTA, or from EDTA-Fe complexes bound to the protein non-specifically following cluster degradation, the stability of the cluster was further investigated in the presence of a chelating resin separated from *Ye*IscR by a semi-permeable membrane. [2Fe–2S] *Ye*IscR was dialysed (3.5 kDa MWCO) against buffer containing Chelex-100 resin (Bio-Rad). Chelex-100 contains the iminodiacetate chelating group and has a high affinity for transition metal ions, and so should chelate any iron released from the Fe–S cluster without being able to interact with the cluster directly.

Samples of *Ye*IscR were taken from the dialysis tubing at increasing time points and the UV–visible absorbance measured, Fig. 6A. This revealed that, under aerobic conditions, ~40 % of clusters were lost over 240 min. This is significantly longer than observed for the EDTA experiment, suggesting that direct interaction between EDTA and the protein/cluster resulted in an enhanced rate of cluster degradation. The Chelex-100 experiments also demonstrate that the iron of the *Ye*IscR [2Fe–2S] cluster is not particularly labile in the absence of a direct interaction.

The effect on *Ye*IscR [2Fe–2S] of the iron chelator ferrozine [44], which has a higher affinity for Fe^{2+} than for Fe^{3+} (log *K* value of 15.5 for Fe^{2+} [45]; undetermined for Fe^{3+} because of autoreduction to Fe^{2+}) was also tested. Ferrozine was added to a final concentration of 0.5 mM to 30 μM [2Fe–2S] *Ye*IscR under anaerobic and aerobic conditions, and the UV–visible absorbance at 562 nm was monitored over time to measure the formation of the Ferrozine-Fe^{2+} complex, Fig. 6B. After 420 min of exposure to 0.5 mM ferrozine under anaerobic conditions, only ~12 % of cluster iron had been released from *Ye*IscR. In comparison, after 420 min under aerobic conditions ~70 % of cluster iron was chelated by ferrozine. Importantly, at 240 min under aerobic conditions, ~40 % cluster iron was complexed by ferrozine. This matches closely the extent of cluster degradation measured using Chelex-100, indicating that ferrozine likely does not interact with the IscR cluster, and so the rate of formation of the iron-ferrozine complex reflects the rate of O_2-mediated decay of the cluster.

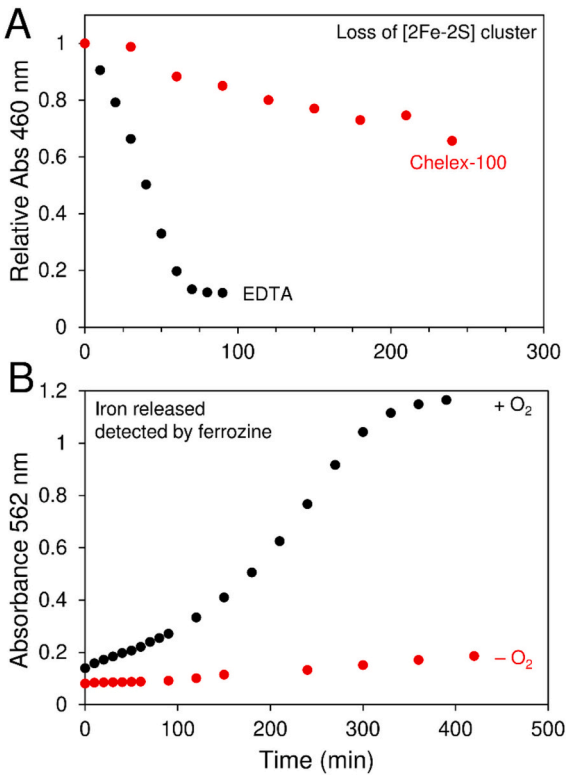

Fig. 6. Chelator-mediated degradation of [2Fe–2S] *Ye*IscR. (A) Change in UV–visible absorbance at 460 nm over time of 30 μM [2Fe–2S] *Ye*IscR (50 mM Tris, 800 mM NaCl, 5 % (*v*/v) glycerol, pH 7.4) separated from Chelex-100 by a semi-permeable membrane (red), or in solution with 1 mM EDTA (black), under aerobic conditions, in a 1 cm pathlength cuvette. (B) Formation of the ferrozine-iron complex over time through the degradation of 30 μM [2Fe–2S] in response to 0.5 mM ferrozine under aerobic (black) and anaerobic (red) conditions. 30 μM [2Fe–2S] *Ye*IscR in 50 mM Tris, 800 mM NaCl, 5 % (v/v) glycerol, pH 8.0. Spectroscopic measurements performed in a 1 cm cuvette. We note that the iron complex of ferrozine detected here is the Fe^{2+} complex, while exposure of IscR to O_2 results in rapid oxidation of the cluster to the all-ferric form. Because reduction of a Fe^{3+}-ferrozine complex is thermodynamically favourable, it can occur readily in complex mixtures with available electrons [43], which is likely the case here. (For interpretation of the references to colour in this figure legend, the reader is referred to the web version of this article.)

Overall, cluster decay, resulting in release of chelatable iron from *Ye*IscR, is very slow and significant release only occurs under aerobic conditions. Thus, the data do not support the hypothesis that IscR functions as a direct iron sensor *in vivo*. Under iron limitation and in the presence of O_2, additional partners appear to be required for the loss of the [2Fe–2S] cluster on a physiologically relevant timescale.

3.6. [2Fe–2S] YeIscR binds type 1 DNA operator sequences

To investigate the DNA-binding properties of *Ye*IscR, and the dependence on the presence of the [2Fe–2S] cluster, DNA-binding assays were performed using a putative type 1 binding site [2] upstream of the *iscR* start codon and the *isc* operon of *Y. enterocolitica.* Such a site is in agreement with the autoregulation of *iscR* described for *E. coli* [1,36]. This promoter region contains two possible IscR binding sites in tandem

(sites A and B), as is also observed in the *E. coli* genome [2].

An 80 bp FAM-tagged oligonucleotide containing both potential IscR binding sites was used for electrophoretic mobility shift assays (EMSAs) (Table S2). Incubation with as-isolated [2Fe–2S] *Ye*IscR demonstrated binding of this form of *Ye*IscR, as evidenced by a shifted DNA-protein band (Fig. 7). Indeed, two shifted bands were observed, suggesting that a mixture of 1 or 2 *Ye*IscR dimers were bound to DNA. The proportion of doubly bound DNA increased as the ratio of [2Fe–2S] *Ye*IscR to DNA increased, and the band presumed to be due to singly bound DNA disappeared after a ratio of ten [2Fe–2S] *Ye*IscR to DNA. Non-specific binding was observed at higher ratios of [2Fe–2S] *Ye*IscR to DNA. Equivalent experiments with apo *Ye*IscR were performed. Binding was observed but only at significantly higher amounts of protein to DNA compared to cluster-bound *Ye*IscR (Fig. 7), indicating that the apo form of *Ye*IscR has a lower affinity.

Binding of *Ye*IscR to each of the two IscR binding sites, termed site A and B, in the *iscR* promoter region, was investigated by native MS. Addition of a 25 bp oligonucleotide, containing IscR binding site A, at an equimolar concentration of the as-isolated [2Fe–2S] *Ye*IscR dimer (DNA: *Ye*IscR dimer = 1:1) resulted in the disappearance of peaks in the 2500–3000 *m/z* region, which correspond to the *Ye*IscR dimer, and additional peaks at 3000–4000 *m/z* were observed that were not present for *Ye*IscR alone (Fig. S8). The deconvoluted mass spectrum contained peaks between 54,000–54,400 Da that correspond to the dimeric forms of *Ye*IscR bound to the site A oligonucleotide, Fig. 8. [2Fe–2S]/[2Fe–2S] dimeric *Ye*IscR was observed bound to the DNA, along with *Ye*IscR containing various cluster breakdown species, including where only one cluster site was occupied in the dimeric protein ([2Fe–2S]/apo *Ye*IscR). These data indicate that degradation of one of the *Ye*IscR Fe–S clusters may not significantly disrupt DNA binding. Unbound *Ye*IscR observed here appeared to be in a Zn-bound form, which presumably has low affinity for DNA.

Apo *Ye*IscR was then mixed with the site A oligonucleotide at the same concentrations as for the [2Fe–2S] form. Some binding of the dimeric apo form to DNA was observed (Fig. 8F); however, a larger proportion of free dimeric protein was observed than for the [2Fe–2S] form (Fig. 8E), in agreement with the EMSAs that indicated that apo IscR has a lower affinity for the type 1 IscR binding site than the [2Fe–2S] form.

Similar experiments were performed with a 25 bp oligonucleotide containing the site B IscR binding site, giving broadly similar data, Fig. S9, suggesting that *Ye*IscR binds with similar affinities to sites A and B.

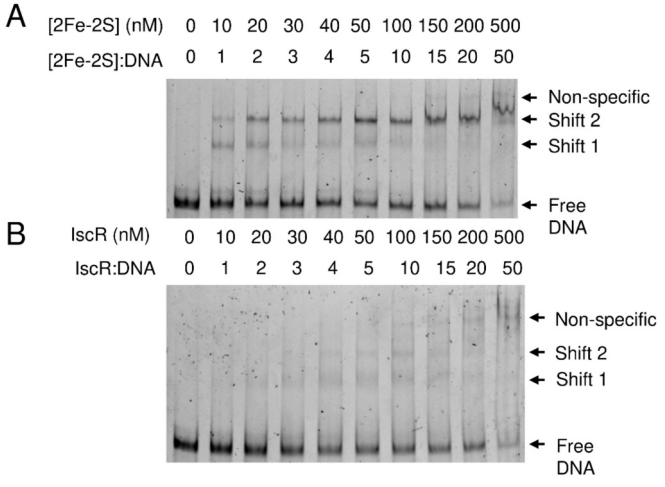

Fig. 7. Electrophoretic mobility shift assay of DNA binding of *Ye*IscR to the *iscR* promoter. EMSA of (A) [2Fe–2S] cluster-bound and (B) apo IscR with 10 nM 80 bp EMSA probe. Ratios between [2Fe–2S] *Ye*IscR or apo *Ye*IscR and the DNA are indicated. Binding reactions were performed in 40 mM Tris, 30 mM NaCl, pH 7.9.

A longer oligonucleotide containing both IscR binding sites, A and B, was added to [2Fe–2S] *Ye*IscR at an equimolar concentration to the [2Fe–2S] cluster concentration (2 DNA:1 *Ye*IscR dimer) and native MS spectra measured. Peaks corresponding to dimeric [2Fe–2S] *Ye*IscR at 2500–3500 *m/z* disappeared upon the addition of DNA, with new peaks appearing at >3500 *m/z* (Fig. S10). Analysis of *m/z* charge states indicated that the main set of peaks at above 3500 *m/z* correspond to one [2Fe–2S]/[2Fe–2S] *Ye*IscR dimer bound to DNA (Fig. S10C), with a second set of lower intensity *m/z* peaks corresponding to two [2Fe–2S]/[2Fe–2S] *Ye*IscR dimers bound to DNA (Fig. S10D). A composite plot of deconvoluted spectra in the regions corresponding to the above species is shown in Fig. S10E. The data indicate that both of the IscR binding sites can be occupied simultaneously; however, the low signal intensity of the doubly IscR-bound DNA prevented further analysis of the data in this case.

3.7. Differences in the DNA binding affinities of oxidised and reduced *Ye*IscR

Surface plasmon resonance (SPR) employing a reusable DNA capture method (ReDCaT) has previously been used to study protein-DNA interactions and to determine the binding affinity, K_d, of the protein for DNA [23,46,47]. SPR using the ReDCaT methodology was thus performed, to gain further quantitative information about the binding of *Ye*IscR to target sequences, as well as more information on the apparent difference in the binding affinities between [2Fe–2S] and apo *Ye*IscR. To facilitate this, samples of IscR at 70–95 % cluster loading were used to minimise contributions from apo IscR and thus simplify the analysis. Binding of reduced $[2Fe–2S]^{1+}$ *Ye*IscR to site A DNA was investigated and normalised responses plotted over the concentration range 0–75 nM. A satisfactory fit could not be obtained using a simple binding equation, and so the Hill equation, which incorporates cooperativity, was used. This resulted in a satisfactory fit, yielding a K_d of ~10 nM and Hill coefficient of ~2 for site A (Table 2). Equivalent SPR experiments were performed to probe binding of $[2Fe–2S]^{1+}$ *Ye*IscR to site B DNA (Fig. 9A and Table 2), demonstrating that *Ye*IscR binds the two sites with the same affinity. Similar experiments were performed with apo IscR, Fig. 9B. Clearly, binding was observed to both sites A and B, but this was weaker than with the cluster-bound form of IscR and fitting gave a K_d of ~120 nM and Hill coefficient of ~1.7 for site A with very similar values for site B (Table 2). Thus, consistent with native MS data, sites A and B both exhibit cluster-dependent binding, as expected for a type 1 IscR binding site.

Given the stability of the *Ye*IscR cluster to environmental cues that lead to de-repression of the *isc* operon, we investigated the effect of cluster oxidation state on the affinity of the protein for binding to type 1 recognition sites. Experiments equivalent to those above but with oxidised $[2Fe–2S]^{2+}$ *Ye*IscR were performed (Fig. 9A), giving a a K_d of ~20 nM and Hill coefficient of ~3 for binding to site A, and similar data for site B (Fig. 9A and Table 2). Thus, the oxidation state of the IscR cluster does affect the affinity for DNA, both in terms of the affinity and the extent of positive cooperativity. This is in contrast to previous reports of *Ec*IscR, where no dependence on cluster oxidation states was observed [25].

4. Discussion

IscR is the master regulator of the Isc Fe–S cluster biogenesis pathway in a wide range of bacteria, and it is now clear that has broader regulatory roles particularly in pathogenic bacteria that exploit the ability of IscR to respond to oxidative/nitrosative stress, and iron availability, such that it functions as a virulence factor [7]. In *Yersinia* species, for example, IscR regulates type III secretion systems that are important for initiating infection [16]. IscR uses its [2Fe–2S] cluster as a sensory module to detect changes in intracellular conditions, resulting in

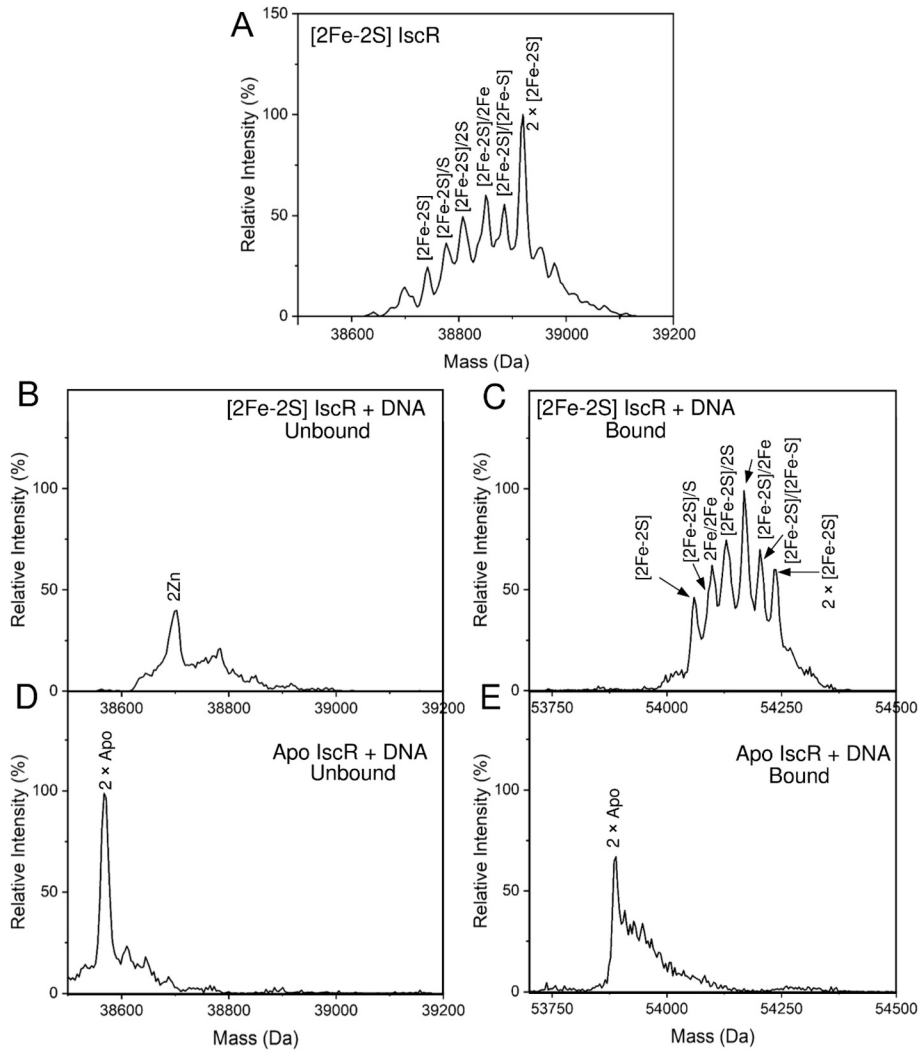

Fig. 8. Binding of *Ye*IscR to site A in the *iscR* promoter. (A) Deconvoluted spectrum of as-isolated [2Fe–2S] *Ye*IscR (8 μM, 4 μM dimer). (B) and (C) As in (A) except that [2Fe–2S] *Ye*IscR was in the presence of site A 25 bp oligonucleotide (4 μM). (D) and (E) apo *Ye*IscR (8 μM) following mixing with site A 25 bp oligonucleotide (4 μM). *Ye*IscR and site A oligonucleotide were exchanged into 100 mM ammonium acetate pH, 8.0 prior to mixing. Note that cluster breakdown species may arise during ionisation.

Table 2
Binding parameters for IscR-DNA complexes.

IscR	Site	Affinity (K_d), nM	Hill coefficient
Red, $[2Fe–2S]^{1+}$	A	9.35 ± 0.22	2.06 ± 0.08
Red, $[2Fe–2S]^{1+}$	B	9.82 ± 0.46	1.70 ± 0.15
Ox, $[2Fe–2S]^{2+}$	A	20.01 ± 1.01	3.08 ± 0.42
Ox, $[2Fe–2S]^{2+}$	B	22.85 ± 1.32	3.88 ± 0.45
Apo	A	119.95 ± 4.36	1.72 ± 0.07
Apo	B	124.38 ± 5.76	1.74 ± 0.08

loss of the cluster and corresponding protein conformational changes that modulate DNA binding. However, a clear understanding of the sensing mechanism, including the identity of the signal that IscR directly responds to, is currently lacking.

Most studies of IscR have been undertaken with the *E. coli* protein; while these have been extremely informative in defining the function of IscR, it is important to broaden studies to include homologs from other organisms so that common functional features can be established. Here, we have characterised the IscR homolog from *Yersinia enterocolitica*, a pathogen related to the causative agent of bubonic plague and itself responsible for most cases of yersiniosis, an infectious disease of the gastrointestinal tract. Anaerobic purification of *Ye*IscR heterologously expressed in *E. coli* resulted in a [2Fe–2S] cluster-containing protein, as indicated by UV–visible spectroscopy and native MS. As isolated, the [2Fe–2S] cluster was found predominately in the reduced, $[2Fe–2S]^{1+}$, state, as previously observed for *E. coli* IscR.

The three conserved cysteine residues of IscR have been shown to be important for cluster binding/activity and are reasonably concluded to be cluster ligands [10,25]. A high-resolution structure of the [2Fe–2S]-bound form of IscR is not yet available, and so unambiguous assignment of the fourth cluster ligand is difficult. Several lines of evidence from studies of *Ec*IscR indicated that highly conserved His107 is a cluster ligand [25]. Alternatively, studies of *Acidithiobacillus ferrooxidans* IscR led to the proposal that Glu43 acts as the fourth ligand to the cluster [48]. However, this residue is located in the DNA-binding domain and is therefore not close to the cluster site. Despite this, it is key for the ability of apo IscR to distinguish between type 1 and type 2 binding sites [26]. Substitution of His107 in *Ye*IscR with either alanine or cysteine resulted in failure to incorporate a [2Fe–2S] cluster, supporting the suggestion that His107 acts as a cluster ligand to one of the iron atoms in the [2Fe–2S] cluster of *Ye*IscR.

Exposure of *Ye*IscR to O_2 resulted in rapid oxidation of the cluster to the $[2Fe–2S]^{2+}$ state. This was followed by degradation of the cluster, but this occurred slowly over a period of many hours. This seems

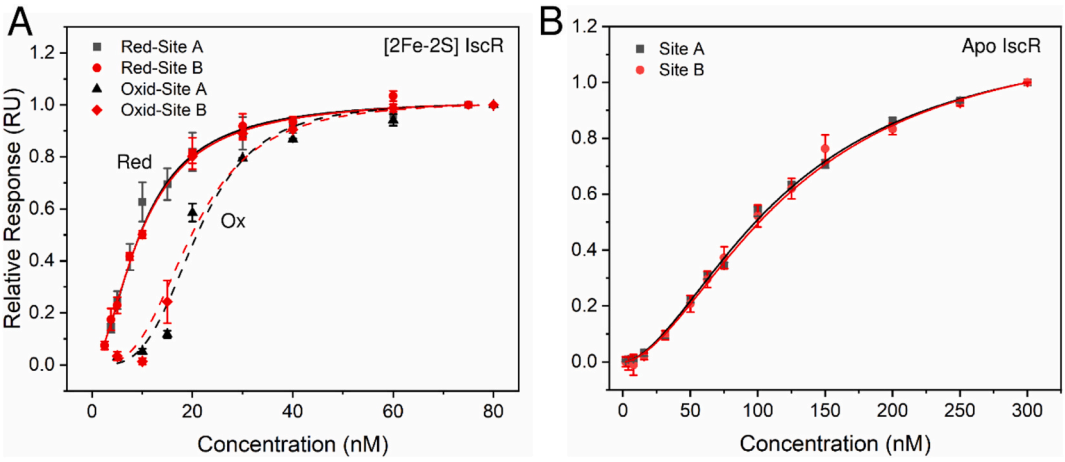

Fig. 9. Affinities of $[2Fe–2S]^{2+}$ (Ox), $[2Fe–2S]^{1+}$ (Red) and apo *Ye*IscR for sites A and B in the *iscR* promoter. (A) Relative response sensogram 5 s before the end of the injection at various concentrations of dimeric [2Fe–2S] *Ye*IscR and with either site A or site B IscR binding motif. The *Ye*IscR cluster was in either the oxidised or reduced state, as indicated. (B) As in (A) but with apo *Ye*IscR binding to site A or site B DNA. Data were fitted using the Hill equation. Each concentration measurement was performed in triplicate. (For interpretation of the references to colour in this figure legend, the reader is referred to the web version of this article.)

inconsistent with *in vivo* data for *E. coli* that showed that a switch to aerobic conditions resulted in a rapid increase in *isc* and *suf* operon expression, indicating the accumulation of IscR in the apo form [2,36]. While type 2 sites can bind IscR in either holo or apo forms, under aerobic conditions where oxidative stress occurs, it is the apo form that accumulates [36]. In some cases, such as the *hya* operon encoding hydrogenase-1 of *E. coli*, it has been shown that the apo form is required for regulation, though the mechanism underlying this is not yet clear [49,50].

The slow rate of cluster loss upon O_2 exposure observed for *Ye*IscR suggests that O_2 itself is not the direct signal for conversion of holo IscR to the apo form *in vivo*. This is consistent with data for *Ec*IscR, from which it was concluded that O_2-mediated cluster loss of IscR is not fast enough to be physiologically important [51]. Oxidation of the cluster upon exposure to O_2 may render IscR more susceptible to cluster loss due to reaction with other signals. ROS can stimulate cluster loss in IscR [8,40], but the data reported here showed that neither hydrogen peroxide nor superoxide had a major effect on the stability of the [2Fe–2S] cluster of *Ye*IscR *in vitro*.

It has been previously shown that low iron conditions can cause derepression of IscR regulated genes in *E. coli*, such as the *isc* operon [8], as well as genes in *Y. pseudotuberculosis* relating to the regulation of the type III secretion system [16]. Iron chelators were used here to simulate low-iron conditions. Under anaerobic conditions, where one of the cluster irons is in the Fe^{2+} state and the other is in the Fe^{3+} state, little degradation of the cluster was observed. Under aerobic conditions, where the cluster would have been in the oxidised (Fe^{3+}/Fe^{3+}) state, degradation did occur, indicating that the oxidised cluster is less stable. However, the rate of cluster degradation was still low. Thus, we conclude that *Ye*IscR does not function as a direct iron sensor through a mechanism involving reversible dissociation of labile iron from the [2Fe–2S] cluster.

The [2Fe–2S] cluster-bound form of *Ye*IscR was able to bind to two adjacent type 1 target sequences found upstream of the *iscR* start site in the *Y. enterocolitica* genome, in agreement with previous work showing that IscR regulates its own transcription [1]. The low nanomolar affinities determined here for binding of [2Fe–2S] *Ye*IscR to the two type 1 sites (A and B) were similar, consistent with equivalent binding at each. The affinities were also similar to those reported for *Ec*IscR [26,36]. For all the DNA-binding assays performed, apo *Ye*IscR bound type 1 IscR sites with a ~ 10-fold lower affinity than the cluster-bound form, consistent with cluster-dependent binding, as shown for *Ec*IscR [1,25,36].

The dependence of DNA binding on the cluster extended beyond just presence. Oxidation state was found to have an effect on both the affinity and the extent of positive cooperativity, such that the presence of the oxidised cluster resulted in weaker binding. The drop in affinity was only ~2-fold but the difference was exacerbated by the increasingly sigmoidal binding curve, such that binding saturations of ~70 % and ~25 % were observed under the same conditions for reduced and oxidised [2Fe–2S] cluster forms of *Ye*IscR (Fig. 9). While this appears to be in contrast to *Ec*IscR, where no dependence of DNA binding on cluster oxidation state was initially reported [36], recent further studies have also identified an oxidation state-dependence of *Ec*IscR binding to type 1 DNA (P. Kiley, personal communication).

The origin of positive cooperativity observed for *Ye*IscR is unclear, but it is also a feature of DNA binding by *E. coli* IscR in both its cluster-bound and apo forms to type 1 and 2 sites, respectively [26]. Positive cooperativity was also observed for RirA, another Rrf2 family regulator [23]. Cooperativity requires the existence of more than one binding site, and the fact that IscR is dimeric is likely to be important here, as are the multiple interactions that occur between the protein and DNA [26]. The increase in cooperativity observed here for the oxidised cluster-bound form of *Ye*IscR suggests that additional interactions between DNA and IscR may arise upon cluster oxidation. That this enhances the difference in binding saturation for oxidised and reduced forms in the lower IscR concentration regime could have physiological significance, but further investigation is needed.

5. Conclusions

The IscR homolog from *Y. enterocolitica* bears many similarities to the *E. coli* protein. It binds a [2Fe–2S] cluster that is isolated in the reduced, 1+, state, and is readily oxidised upon exposure to O_2 or other oxidants. While the presence of O_2 destabilised the cluster, leading to eventual loss, this occurred very slowly. The IscR cluster was also relatively insensitive to other ROS, and to iron chelators, indicating that the cluster itself is not labile or generally very reactive, except to oxidation state change. The presence of the cluster leads to a significant (~10-fold) increase in affinity for type 1 DNA sites, similar to that reported for *E. coli* IscR, and likely sufficient to be physiologically important. Unexpectedly, and distinct from earlier reports for the *E. coli* protein, the oxidation state of the cluster was also found to be important for DNA binding, with a reduction in affinity, but an increase in the extent of positive cooperativity observed upon cluster oxidation. This suggests that exposure to oxidative stress that overcomes the usually reducing

environment of the cell cytoplasm might be sufficient to result in a transcriptional response [52]. Such a response could be particularly important for an invading pathogen that will encounter oxidative stress as it tries to establish infection, because cluster oxidation is effectively instantaneous, permitting an immediate transcriptional response to oxidative stress conditions. However, oxidation state dependence of DNA binding would not alone explain the accumulation of apo IscR that is needed for activation of the *suf* operon. Thus, further investigations of the stability of the IscR [2Fe–2S] cluster, particularly in its oxidised state, and in DNA-bound form, are needed in order to understand how loss of the cluster occurs on a physiologically relevant timescale. Such studies are in progress.

CRediT authorship contribution statement

Elizabeth Gray: Writing – original draft, Investigation, Formal analysis, Conceptualization. **Miaomiao Gao:** Investigation, Formal analysis, Conceptualization. **Justin M. Bradley:** Supervision, Investigation. **Jason C. Crack:** Writing – review & editing, Supervision, Conceptualization. **Nick E. Le Brun:** Writing – review & editing, Writing – original draft, Supervision, Funding acquisition, Conceptualization.

Funding

This work was supported by the award of a Biotechnology and Biological Sciences Research Council Norwich Research Park Doctoral Training Partnership PhD studentship to EG, BBSRC grant BB/V006851/1 and the Royal Society International Exchange grant IEC\R2\170168. BBSRC grant BB/R013578/1 supported the purchase of an ICP-QQQ-MS instrument. This article is based upon work from COST Action FeS-ImmChemNet, CA21115, supported by COST (European Cooperation in Science and Technology).

Declaration of competing interest

The authors declare that they have no known competing financial interests or personal relationships that could have appeared to influence the work reported in this paper.

Acknowledgements

We thank UEA Science Faculty Analytical Facility for access to SPR facilities, and UEA for the initial purchase and subsequent maintenance of the Q-TOF MS instrument. We thank Dr. Myles Cheesman (UEA) for access to the CD spectrometer, and Prof. Patricia Kiley and Dr. Erin Mettert (University of Wisconsin, USA) for helpful discussions.

Appendix A. Supplementary data

Supplementary data to this article can be found online at https://doi.org/10.1016/j.jinorgbio.2025.113011.

Data availability

Data supporting the conclusions of this study are available in the main paper with additional experimental data given in the Supplementary Data. All data are available from the corresponding author upon request.

References

[1] C.J. Schwartz, J.L. Giel, T. Patschkowski, C. Luther, F.J. Ruzicka, H. Beinert, P. J. Kiley, IscR, an Fe-S cluster-containing transcription factor, represses expression of *Escherichia coli* genes encoding Fe-S cluster assembly proteins, Proc. Natl. Acad. Sci. USA 98 (2001) 14895–14900.

[2] J.L. Giel, D. Rodionov, M. Liu, F.R. Blattner, P.J. Kiley, IscR-dependent gene expression links iron-sulphur cluster assembly to the control of O_2-regulated genes in *Escherichia coli*, Mol. Microbiol. 60 (2006) 1058–1075.

[3] G. Rincon-Enriquez, P. Crete, F. Barras, B. Py, Biogenesis of Fe/S proteins and pathogenicity: IscR plays a key role in allowing *Erwinia chrysanthemi* to adapt to hostile conditions, Mol. Microbiol. 67 (2008) 1257–1273.

[4] J. Zeng, K. Zhang, J. Liu, G. Qiu, Expression, purification, and characterization of iron-sulfur cluster assembly regulator IscR from *Acidithiobacillus ferrooxidans*, J. Microbiol. Biotechnol. 18 (2008) 1672–1677.

[5] S.H. Kim, B.Y. Lee, G.W. Lau, Y.H. Cho, IscR modulates catalase a (KatA) activity, peroxide resistance and full virulence of *Pseudomonas aeruginosa* PA14, J. Microbiol. Biotechnol. 19 (2009) 1520–1526.

[6] J.G. Lim, S.H. Choi, IscR is a global regulator essential for pathogenesis of *Vibrio vulnificus* and induced by host cells, Infect. Immun. 82 (2014) 569–578.

[7] E.L. Mettert, P.J. Kiley, Fe-S cluster homeostasis and beyond: the multifaceted roles of IscR, Biochim. Biophys. Acta, Mol. Cell Res. 1871 (6) (2024) 119749.

[8] F.W. Outten, O. Djaman, G. Storz, A suf operon requirement for Fe-S cluster assembly during iron starvation in *Escherichia coli*, Mol. Microbiol. 52 (2004) 861–872.

[9] K.C. Lee, W.S. Yeo, J.H. Roe, Oxidant-responsive induction of the *suf* operon, encoding a Fe-S assembly system, through Fur and IscR in *Escherichia coli*, J. Bacteriol. 190 (2008) 8244–8247.

[10] W.S. Yeo, J.H. Lee, K.C. Lee, J.H. Roe, IscR acts as an activator in response to oxidative stress for the *suf* operon encoding Fe-S assembly proteins, Mol. Microbiol. 61 (2006) 206–218.

[11] E.L. Mettert, P.J. Kiley, Coordinate regulation of the Suf and Isc Fe-S cluster biogenesis pathways by IscR is essential for viability of *Escherichia coli*, J. Bacteriol. 196 (2014) 4315–4323.

[12] J.A. Seabaugh, D.M. Anderson, Pathogenicity and virulence of *Yersinia*, Virulence 15 (2024) 2316439.

[13] X. Fang, L. Kang, Y.F. Qiu, Z.S. Li, Y. Bai, *Yersinia enterocolitica* in Crohn's disease, Front. Cell. Infect. Microbiol. 13 (2023) 1129996.

[14] D. Balderas, E. Mettert, H.N. Lam, R. Banerjee, T. Gverzdys, P. Alvarez, G. Saarunya, N. Tanner, A. Zoubedi, Y. Wei, P.J. Kiley, V. Auerbuch, Genome scale analysis reveals IscR directly and indirectly regulates virulence factor genes in pathogenic *Yersinia*, mBio 12 (2021) e0063321.

[15] H.K. Miller, L. Kwuan, L. Schwiesow, D.L. Bernick, E. Mettert, H.A. Ramirez, J. M. Ragle, P.P. Chan, P.J. Kiley, T.M. Lowe, V. Auerbuch, IscR is essential for *Yersinia pseudotuberculosis* type III secretion and virulence, PLoS Pathog. 10 (2014) e1004194.

[16] D. Hooker-Romero, E. Mettert, L. Schwiesow, D. Balderas, P.A. Alvarez, A. Kicin, A. L. Gonzalez, G.V. Plano, P.J. Kiley, V. Auerbuch, Iron availability and oxygen tension regulate the *Yersinia* Ysc type III secretion system to enable disseminated infection, PLoS Pathog. 15 (12) (2019) e1008001.

[17] T. Perez-Ruiz, C. Martinez-Lozano, V. Tomas, J. Fenoll, Determination of proteins in serum by fluorescence quenching of rose bengal using the stopped-flow mixing technique, Analyst 125 (2000) 507–510.

[18] J.C. Crack, J. Green, A.J. Thomson, N.E. Le Brun, Techniques for the production, isolation, and analysis of iron-sulfur proteins, Methods Mol. Biol. 1122 (2014) 33–48.

[19] J.C. Crack, N.E. Le Brun, Native mass spectrometry of iron-sulfur proteins, Methods Mol. Biol. 2353 (2021) 231–258.

[20] M.T. Marty, A.J. Baldwin, E.G. Marklund, G.K. Hochberg, J.L. Benesch, C. V. Robinson, Bayesian deconvolution of mass and ion mobility spectra: from binary interactions to polydisperse ensembles, Anal. Chem. 87 (2015) 4370–4376.

[21] L.M. Hellman, M.G. Fried, Electrophoretic mobility shift assay (EMSA) for detecting protein-nucleic acid interactions, Nat. Protoc. 2 (2007) 1849–1861.

[22] C.E. Stevenson, A. Assaad, G. Chandra, T.B. Le, S.J. Greive, M.J. Bibb, D. M. Lawson, Investigation of DNA sequence recognition by a streptomycete MarR family transcriptional regulator through surface plasmon resonance and X-ray crystallography, Nucleic Acids Res. 41 (2013) 7009–7022.

[23] E. Gray, M.Y.Y. Stewart, L. Hanwell, J.C. Crack, R. Devine, C.E.M. Stevenson, A. Volbeda, A.W.B. Johnston, J.C. Fontecilla-Camps, M.I. Hutchings, J.D. Todd, N. E. Le Brun, Stabilisation of the RirA [4Fe-4S] cluster results in loss of iron-sensing function, Chem. Sci. 14 (2023) 9744–9758.

[24] S.A. Freibert, B.D. Weiler, E. Bill, A.J. Pierik, U. Muhlenhoff, R. Lill, Biochemical reconstitution and spectroscopic analysis of iron-sulfur proteins, Methods Enzymol. 599 (2018) 197–226.

[25] A.S. Fleischhacker, A. Stubna, K.L. Hsueh, Y. Guo, S.J. Teter, J.C. Rose, T. C. Brunold, J.L. Markley, E. Munck, P.J. Kiley, Characterization of the [2Fe-2S] cluster of *Escherichia coli* transcription factor IscR, Biochemistry 51 (2012) 4453–4462.

[26] S. Rajagopalan, S.J. Teter, P.H. Zwart, R.G. Brennan, K.J. Phillips, P.J. Kiley, Studies of IscR reveal a unique mechanism for metal-dependent regulation of DNA binding specificity, Nat. Struct. Mol. Biol. 20 (2013) 740–747.

[27] J.A. Santos, N. Alonso-Garcia, S. Macedo-Ribeiro, P.J. Pereira, The unique regulation of iron-sulfur cluster biogenesis in a gram-positive bacterium, Proc. Natl. Acad. Sci. USA 111 (2014) E2251–E2260.

[28] M.T. Pellicer Martinez, A.B. Martinez, J.C. Crack, J.D. Holmes, D.A. Svistunenko, A.W.B. Johnston, M.R. Cheesman, J.D. Todd, N.E. Le Brun, Sensing iron availability via the fragile [4Fe-4S] cluster of the bacterial transcriptional repressor RirA, Chem. Sci. 8 (2017) 8451–8463.

[29] W. Shepard, O. Soutourina, E. Courtois, P. England, A. Haouz, I. Martin-Verstraete, Insights into the Rrf2 repressor family - the structure of CymR, the global cysteine regulator of *Bacillus subtilis*, FEBS J. 278 (2011) 2689–2701.

[30] A. Volbeda, E.L. Dodd, C. Darnault, J.C. Crack, O. Renoux, M.I. Hutchings, N.E. Le Brun, J.C. Fontecilla-Camps, Crystal structures of the NO sensor NsrR reveal how its iron-sulfur cluster modulates DNA binding, Nat. Commun. 8 (2017) 15052.
[31] A. Volbeda, M.T.P. Martinez, J.C. Crack, P. Amara, O. Gigarel, J.T. Munnoch, M. I. Hutchings, C. Darnault, N.E. Le Brun, J.C. Fontecilla-Camps, Crystal structure of the transcription regulator RsrR reveals a [2Fe-2S] cluster coordinated by Cys, Glu, and his residues, J. Am. Chem. Soc. 141 (2019) 2367–2375.
[32] J.C. Crack, J. Munnoch, E.L. Dodd, F. Knowles, M.M. Al Bassam, S. Kamali, A. A. Holland, S.P. Cramer, C.J. Hamilton, M.K. Johnson, A.J. Thomson, M. I. Hutchings, N.E. Le Brun, NsrR from *Streptomyces coelicolor* is a nitric oxide-sensing [4Fe-4S] cluster protein with a specialized regulatory function, J. Biol. Chem. 290 (2015) 12689–12704.
[33] J.T. Munnoch, M.T. Martinez, D.A. Svistunenko, J.C. Crack, N.E. Le Brun, M. I. Hutchings, Characterization of a putative NsrR homologue in *Streptomyces venezuelae* reveals a new member of the Rrf2 superfamily, Sci. Rep. 6 (2016) 31597.
[34] J.C. Crack, J. Green, A.J. Thomson, N.E. Le Brun, Iron-sulfur clusters as biological sensors: the chemistry of reactions with molecular oxygen and nitric oxide, Acc. Chem. Res. 47 (2014) 3196–3205.
[35] E.L. Mettert, P.J. Kiley, Fe-S proteins that regulate gene expression, Biochim. Biophys. Acta 2015 (1853) 1284–1293.
[36] J.L. Giel, A.D. Nesbit, E.L. Mettert, A.S. Fleischhacker, B.T. Wanta, P.J. Kiley, Regulation of iron-sulphur cluster homeostasis through transcriptional control of the Isc pathway by [2Fe-2S]-IscR in *Escherichia coli*, Mol. Microbiol. 87 (2013) 478–492.
[37] V.R. Sutton, E.L. Mettert, H. Beinert, P.J. Kiley, Kinetic analysis of the oxidative conversion of the $[4Fe\text{-}4S]^{2+}$ cluster of FNR to a $[2Fe\text{-}2S]^{2+}$ cluster, J. Bacteriol. 186 (2004) 8018–8025.
[38] S. Jang, J.A. Imlay, Micromolar intracellular hydrogen peroxide disrupts metabolism by damaging iron-sulfur enzymes, J. Biol. Chem. 282 (2007) 929–937.
[39] J.A. Imlay, The molecular mechanisms and physiological consequences of oxidative stress: lessons from a model bacterium, Nat. Rev. Microbiol. 11 (2013) 443–454.
[40] A. Romsang, J. Duang-Nkern, P. Leesukon, K. Saninjuk, P. Vattanaviboon, S. Mongkolsuk, The iron-Sulphur cluster biosynthesis regulator IscR contributes to iron homeostasis and resistance to oxidants in *Pseudomonas aeruginosa*, PLoS One 9 (2014) e86763.
[41] H.A. Flaschka, The stability constants of EDTA complexes, in: H.A. Flaschka, B. Naiman (Eds.), EDTA Titrations: An Introduction to Theory and Practice, Pergamon Press, 1959, pp. 24–30.
[42] M.T. Pellicer Martinez, J.C. Crack, M.Y. Stewart, J.M. Bradley, D.A. Svistunenko, A. W. Johnston, M.R. Cheesman, J.D. Todd, N.E. Le Brun, Mechanisms of iron- and O_2-sensing by the [4Fe-4S] cluster of the global iron regulator RirA, Elife 8 (2019) e47804.
[43] J. Im, J. Lee, F.E. Loffler, Interference of ferric ions with ferrous iron quantification using the ferrozine assay, J. Microbiol. Methods 95 (2013) 366–367.
[44] W.W. Fish, Rapid colorimetric micromethod for the quantitation of complexed iron in biological samples, Methods Enzymol. 158 (1988) 357–364.
[45] C.R. Gibbs, Characterization and application of ferrozine iron reagent as a ferrous iron indicator, Anal. Chem. 48 (1976) 1197–1201.
[46] P.G. Stockley, B. Persson, Surface plasmon resonance assays of DNA-protein interactions, Methods Mol. Biol. 543 (2009) 653–669.
[47] H.F. Teh, W.Y. Peh, X. Su, J.S. Thomsen, Characterization of protein–DNA interactions using surface plasmon resonance spectroscopy with various assay schemes, Biochemistry 46 (2007) 2127–2135.
[48] J. Zeng, X. Zhang, Y. Wang, C. Ai, Q. Liu, G. Qiu, Glu43 is an essential residue for coordinating the $[Fe_2S_2]$ cluster of IscR from *Acidithiobacillus ferrooxidans*, FEBS Lett. 582 (2008) 3889–3892.
[49] A.D. Nesbit, A.S. Fleischhacker, S.J. Teter, P.J. Kiley, ArcA and AppY antagonize IscR repression of hydrogenase-1 expression under anaerobic conditions, revealing a novel mode of O_2 regulation of gene expression in *Escherichia coli*, J. Bacteriol. 194 (2012) 6892–6899.
[50] A.D. Nesbit, J.L. Giel, J.C. Rose, P.J. Kiley, Sequence-specific binding to a subset of IscR-regulated promoters does not require IscR Fe-S cluster ligation, J. Mol. Biol. 387 (2009) 28–41.
[51] E.L. Mettert, N.T. Perna, P.J. Kiley, Sensing the cellular Fe-S cluster demand: A structural, functional, and phylogenetic overview of *Escherichia coli* IscR, in: T. A. Rouault (Ed.), Iron-Sulfur Clusters in Chemistry and Biology, De Gruyter, 2014.
[52] J.C. Crack, P. Amara, A. Volbeda, J.M. Mouesca, R. Rohac, M.T. Pellicer Martinez, C.Y. Huang, O. Gigarel, C. Rinaldi, N.E. Le Brun, J.C. Fontecilla-Camps, Electron and proton transfers modulate DNA binding by the transcription regulator RsrR, J. Am. Chem. Soc. 142 (2020) 5104–5116.